In-time optical wireless ammonia (NH_3) sensing using C+L band broadband source

HSIN-CHE LEE, YAN-TING LIN, DONG-CHANG LI, SHIEN-KUEI LIAW*
Department of Electronic and Computer Engineering, National Taiwan University of Science and Technology, Taipei 106, Taiwan

In-time optical wireless sensing Ammonia (NH3) using a broadband light source is proposed. By selecting a broadband light source, the emission spectrum partially overlaps with the absorption spectrum with gas under test. In our example, a C+L band light source operating in the wavelength range of 1535 nm to 1605 nm is used. The induced loss of the sensitivity by NH_3 concentration is 0.0016 mW/ppm at 1531.13 nm.

(Received April 5, 2019; accepted February 17, 2020)

Keywords: Free space optical communication, indoor optical wireless communication, Erbium doped fiber amplifier, gas sensing.

1. Introduction

Atmospheric ammonia (NH_3) stands in the third place for abundant nitrogen spices and a crucial atmospheric base. Therefore, the measurement of NH_3 is an important factor in learning aerosol nucleation and new particle formation [1], [2]. At room temperature, Ammonia (NH_3) is colorless, with an irritating odor, it is lighter than air. The human body can sense 5.3 ppm of NH_3. Due to the extremely high solubility of ammonia, it can easily adhere on human skin and conjunctiva so as to induce irritation. The NH_3 is mainly produced by agriculture, animal husbandry and transportation. The main source of ammonia at home is from the use of concrete containing urea and ammonia, such as the wall, the interior decoration materials coated with additives and brightener. These construction materials release ammonia when the environmental temperature and/or the humidity changes. Thus, it will increase the ammonia concentration. Growing plants can result in the use of fertilizer as well as fertilizer production [3]. Among them, the ammonia fertilizer takes the major consumption proportion [4]; however, only about 40% of the ammonia fertilizer is effectively absorbed by crops [5]. The residual of unused fertilizers penetrates into soil, water and atmosphere. They cause big environmental problems such as soil acidification, fog haze and water eutrophication, and therefore lead to human disease, economic loss, and so on [6]. The drawback of ammonia (NH_3) volatilization includes nitrogen loss [7]; therefore, improving the efficiency of ammonia fertilizer utilization is important [8]. Currently, there are some methods proposed to reduce the ammonia volatilization [9]; on the other hand, a precise and real-time ammonia monitoring technique is also a critical issue [10]. In this paper, a wireless optical communication architecture is applied for gas sensing. Different ammonia concentration results in different light source absorption, and the received spectrum is observed by an optical spectrum analyzer. We use method one to pin down the gas leakage so as to immediately set off an alarm to prevent danger.

2. Beer's law and ammonia

In general, different gases have different absorption spectra. Based on the Beer's law [11]. When a certain light wavelength with absorption characteristic at this region passes through gas, the light power decreases accordingly. The chamber's length is b (in cm), P_0 is the incident light intensity, and P is the light intensity after passing through the gas chamber, as shown in Fig.1.

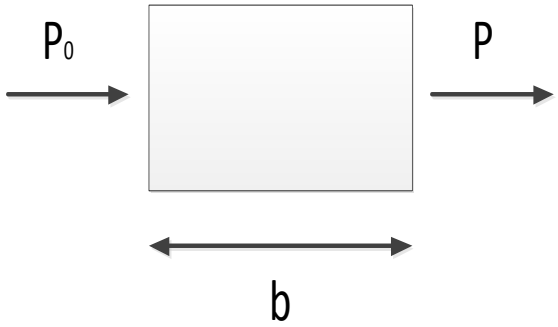

Fig. 1 Definition of the Beer's law uses an absorbed gas inside the chamber

The definition of absorbance (*A*) is the ratio of P and P_0, and they adopt the logarithm scale. The equation is shown as followed:

$$A = -log\left(\frac{P}{P_0}\right) = -log\, T \quad (1)$$

where A is light absorption and T is light transmittance. The relationship between gas concentration and light absorbance can be described by Beer's law as followed [12]:

$$A = \varepsilon bc \quad (2)$$

where ε is the gas molar absorption coefficient (M-1cm-1) to be tested; b is the length (cm) of the gas chamber: c is the gas concentration (*mol/L*, M). From formula one, we know that the gas concentration in a specific wavelength range is proportional to the light absorption. The C+L band light source, ranging from 1520 to 1610 nm, is used in the experiment. Prior to the experiment, the high-resolution transmission molecular absorption database-(HITRAN) was used to query and simulate the spectral absorption of ammonia in such wavelength range as shown in Fig. 2 [13].

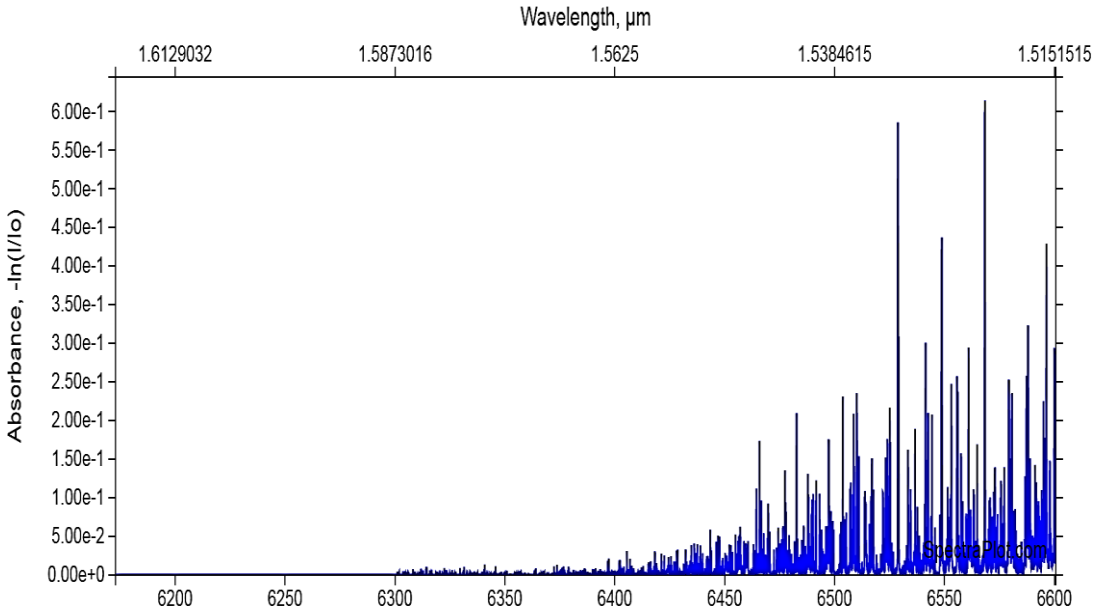

Fig. 2. The simulation spectra shows ammonia gas absorption in wavelength range of 1515- to 1612 nm. [13]

We find that ammonia gas has different absorption in the wavelength range of 1520 nm to 1562 nm. The wavelength range of 1527 nm and 1531 nm creates strong absorption while there is nearly no absorption between 1565 nm and 1610 nm. In this experiment, the gas chamber is vacuumed to begin with. Then the ammonia gas is used to fill in the gas chamber gradually, which causes gas pressure to vary inside the gas chamber. Based on the ideal gas equation [14], the ammonia concentration in the gas chamber can be obtained. The detected gas pressure is used to estimate the ammonia concentration inside the gas chamber.

$$PV=nRT \quad (3)$$

where P is the gas pressure (atm), V is the gas volume (L), n is the gas mole number (mol), R is the ideal gas constant (atm-L/mole-K), and T is the absolute temperature (K). After obtaining the mole number of ammonia inside the gas chamber, the volumetric molar concentration of ammonia can be calculated. The volume molarity (M) is defined as the number of gas moles per cubic meter. It can be expressed as:

$$M = \frac{n}{V} \quad (4)$$

where n is the volume of mole and V is the gas volume (L). The data is converted into the commonly used representation of parts per million (ppm), which is defined as solute in solution per liter. In this experiment, the gas pressure in chamber ranges from 0.3- to 1.5 atm, so we measure the absorption spectrum of ammonia gas at 0.3-, 0.9- and 1.5 atmosphere. After that, we convert the measured pressure value into parts per million, the calculation result is summarized in Table 1.

Table 1. The NH_3 density under different pressure

atm	(M=mol/L)	(ppm=mg/L)
0.3	0.012	206
0.9	0.037	646
1.5	0.060	1027

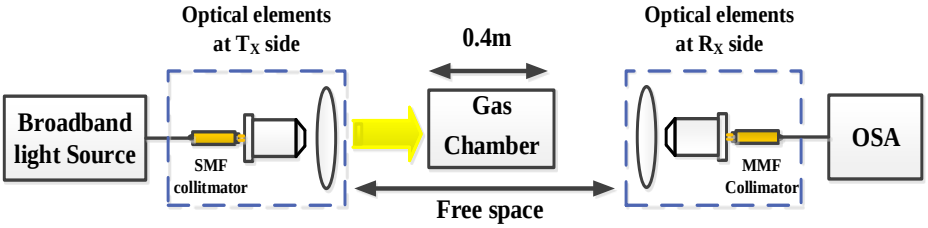

Fig. 3. Gas detection in an experimental architecture diagram (color online)

3. Experimental setup

The experimental setup, which is shown in Fig. 3, includes broadband source, transmitter, gas chamber and receiver. The gas chamber has an outside length, width and height of 40 cm, 20 cm and 10 cm, respectively, and an inner length of 37 cm and a thickness of 1.5 cm. Then the broadband source transmits the gas chamber and it is partially absorbed by the gas at certain wavelength. On the receiving side, there are a convex len, a 10x objective len and a multimode fiber collimator to receive the residual optical power. Before immersing the Ammonia in different pressure, we set the gas chamber in zero pressure. There is a pair of five-axis moving optical stage to optimize the optical path so as to reduce the transmission loss. After completing the alignment step of the optical path, the Ammonia is then added into the gas chamber. At the chamber interface, the broadband source is reflecting due to the variation of refractive index and/or divergence angle, or it refracts at the chamber interfaces due to non-uniformity. It is necessary to fine-tune the five-axis optical stage pair.

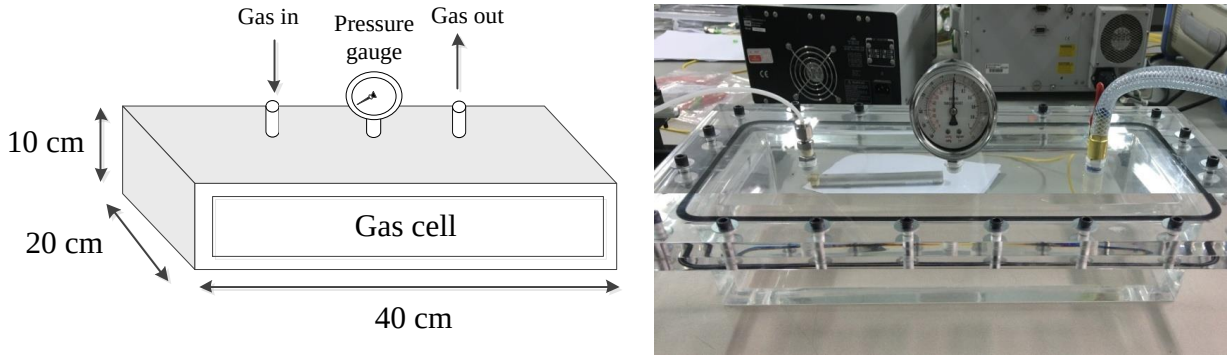

(a) *(b)*

Fig. 4. (a) The designed gas chamber and (b) the customer-designed gas chamber

After that, the Ammonia gas is put into the 40-cm length gas chamber gradually. As discussed in the previous paragraph, the specific wavelength is absorbed by the Ammonia gas. The gas chamber we use can withstand a maximum pressure of 1 kg/cm^2, and it is as shown in Fig. 4(a) and Fig. 4(b).

In order to confirm that the broadband source has the same power decay for the whole band after passing through the free space and penetrating the gas chamber, an optical spectrum analyzer is used to measure the power and change of the spectra. The result of the measurement is shown in Fig. 5 (a). The black line represents the original spectra of the C+L band light source, red line is the light spectrum after 1 meter transmission in free space, and green line is the light spectrum after penetrating the gas chamber. Compared to the black curve, the light power of red and

green curves decreases relatively smoother.

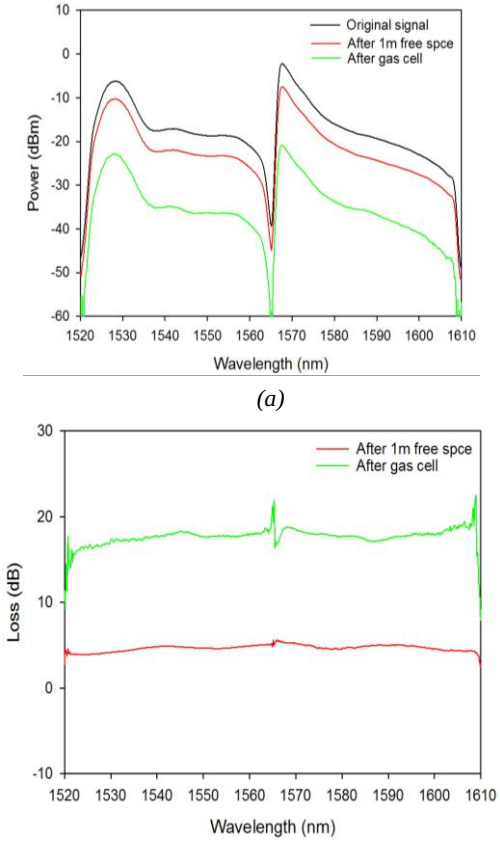

Fig. 5(a) Different spectra of a broadband source, and (b) the light power decreases spectra when compared with original light source.

In Fig. 5(a), we found that the extra optical loss is up to 10 dB after inserting the gas chamber in between the free space path. The extra loss includes four interface loss of air/chamber, misalignment loss because light source path and chamber when offset from the orthogonal direction. Nevertheless, it did not affect the experimental results because both of two effects just induced optical loss. In Fig. 5(b), we deduce the light power between black curve and red curve, and also deduce the black curve and green curve. We find that the red curve has lower absorption than that of the green curve.

4. Results and discussion

Fig. 6 (a) is the light absorption spectra measured under different ammonia concentrations. The black line indicates when the gas chamber is vacuumed. As the ammonia gas gradually increases, the power of light source decreases accordingly in the region of 1520- to 1610 nm. The absorption spectra of NH_3 in C band has multiple little absorption peaks. The absorption spectra in L band is smoother than that in C band. Fig. 6(b) shows the wavelength of optical power loss at different ammonia concentrations. Up to five wavelengths are measured and drawn in curves.

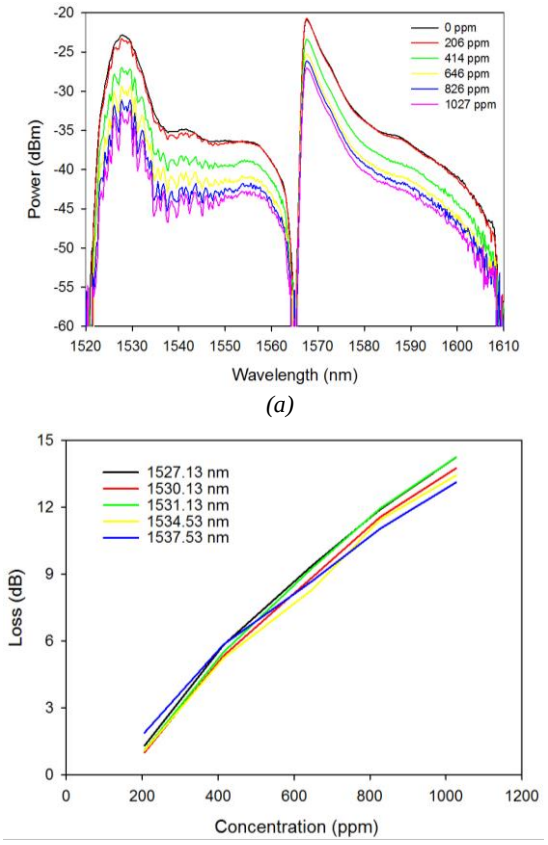

Fig. 6(a) Absorption spectra at different ammonia concentrations, (b) wavelength optical power loss at different ammonia concentration

As the ammonia concentration increases, the light source at the five wavelengths are liner decreased in the optical power. According to Beer's law, the ammonia gas concentration has linear relationship to light power absorption. To have repeatable and reliable experimental data, all measurements were done at room temperature of 24-25C.

Fig. 7(a) shows the absorbance at 1527.13 nm under different ammonia concentrations. The sensitivity is 0.0016 mW/ppm and the linearity R2 is 0.9862. Similarly, Fig. 7(b) shows the absorbance at 1531.13m under different ammonia concentrations. The sensitivity is 0.0016 mW/ppm and the linearity R2 is 0.9881. Overall, the experimental results have high linearity and sensitivity.

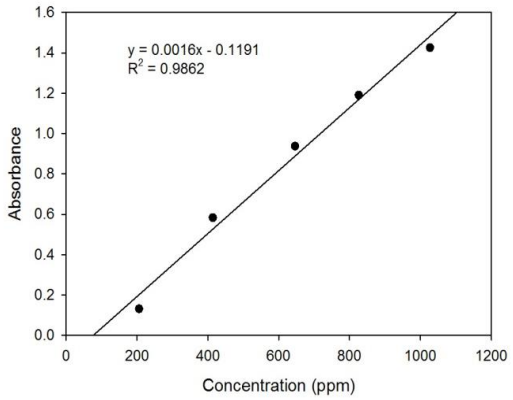

(a)

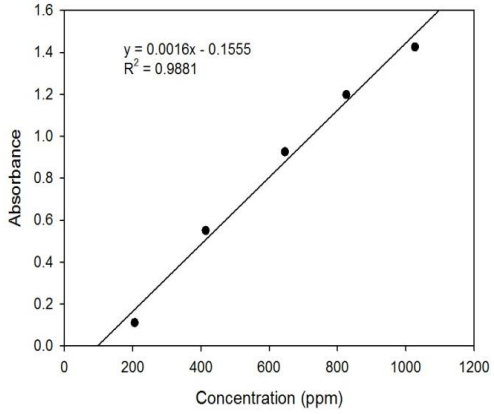

(b)

Fig. 7 Absorption at a wavelength of (a) 1527.13 nm and (b) 1531.13 at different ammonia concentrations

To reduce the cost and size, a C band semiconductor optical amplifier (SOA) may be used to replace the broadband light source; also, a bandpass filter, locks at high absorption wavelength of NH_3 may integrate with a photo detector to replace the optical spectrum analyzer.

5. Conclusion

In this paper, the C+L band broadband source is absorbed by the ammonia with concentration from 206- to 1027 ppm. We find that the phenomenon of high absorption occurs in the wavelength range of 1520- to 1562 nm. At 1531.13 nm, the absorption sensitivity against concentration change is 0.0016 mW/ppm and the linearity R^2 is 0.9881. The absorbance has good linearity and it's very sensitive to the change of ammonia concentration.

Acknowledgements

The work is supported in part by MOST of Taiwan under Grand Numbers MOST 108-2622-8-011 -003 -TE1 and MOST 107-2218-E-011 -020 -. The authors would like to thank Ms. Yi-Wen Chen's help and optical networking laboratory of NTUST for equipment support.

References

[1] J. L. Camas-Anzueto, A. E. Aguilar-Castillejos, J. H. Castañón-González, M. C. Lujpán-Hidalgo, H. R. Hernández De León, R. Mota Grajales, Opt. Lasers Eng. **60**, 38 (2014).
[2] L. Clarisse, C. Clerbaux, F. Dentener, D. Hurtmans, P. F. Coheur, Nat. Geosci **2**(7), 479 (2009).
[3] T. L. Roberts, Better Crop **93**(2), 12 (2009).
[4] C. W. Gellings, K. E. Parmenter, Energy use and conservation of energy - Vol II, Energy efficiency in fertilizer production and use, Encycl. Life Support Syst., (2004).
[5] H. Fan, S.-S. Jiang, Y. Wei, J.-Y. Jiang, Huan jing ke xue= Huanjing kexue **37**(8), 2906 (2016).
[6] L. Clarisse, C. Clerbaux, F. Dentener, D. Hurtmans, P. F. Coheur, Nat. Geosci. **2**(7), 479 (2009).
[7] L. Wu et al., Nature **514**(7523), 486 (2014).
[8] Y. Wu et al., Sensors Actuators B Chem. **286**, 62 (2019).
[9] X. Sun, T. Zhong, L. Zhang, K. Zhang, W. Wu, Sci. Total Environ. **660**, 512 (2019).
[10] X. Yang et al., Opt. Lasers Eng. **115**, 243 (2018).
[11] T. G. Mayerhöfer, J.Popp, Chem. Phys. Chem. **20(**4), 511 (2019).
[12] M. Lancaster, Phys. Sci. Basis **53**, 1 (1989).
[13] HITRANonline, https://hitran.org/.
[14] A. L. Myers, J. M. Prausnitz, AIChE J. **11**(1), 121 (1965).

*Corresponding author: peterskliaw@gmail.com